11C-Methionine-PET in multiple myeloma: a combined study from two different institutions

Constantin Lapa, Maria J. Garcia-Velloso, Katharina Lückerath, Samuel Samnick, Martin Schreder, Paula Rodriguez Otero, Jan-Stefan Schmid, Ken Herrmann, Stefan Knop, Andreas K. Buck, Hermann Einsele, Jesus San-Miguel, Klaus Martin Kortüm

Angaben zur Veröffentlichung / Publication details:

Lapa, Constantin, Maria J. Garcia-Velloso, Katharina Lückerath, Samuel Samnick, Martin Schreder, Paula Rodriguez Otero, Jan-Stefan Schmid, et al. 2017. "11C-Methionine-PET in multiple myeloma: a combined study from two different institutions." *Theranostics* 7 (11): 2956–64. https://doi.org/10.7150/thno.20491.

IVYSPRING INTERNATIONAL PUBLISHER

Theranostics

2017; 7(11): 2956-2964. doi: 10.7150/thno.20491

Research Paper

^{11}C-Methionine-PET in Multiple Myeloma: A Combined Study from Two Different Institutions

Constantin Lapa[1*✉], Maria J. Garcia-Velloso[2*], Katharina Lückerath[1], Samuel Samnick[1], Martin Schreder[3], Paula Rodriguez Otero[2], Jan-Stefan Schmid[1], Ken Herrmann[1,4], Stefan Knop[3], Andreas K. Buck[1], Hermann Einsele[3], Jesus San-Miguel[2#], Klaus Martin Kortüm[3#]

1. University Hospital Würzburg, Department of Nuclear Medicine, Würzburg, Germany
2. Clinica Universidad de Navarra, Center of Applied Medical Research, Navarra Institute for Health Research (CIMA). IDISNA, Pamplona, Spain
3. University Hospital Würzburg, Department of Hematology and Oncology, Würzburg, Germany
4. University Hospital Essen, Department of Nuclear Medicine, Essen, Germany

* equal contribution

# equal contribution

✉ Corresponding author: Constantin Lapa, MD, University Hospital Würzburg, Department of Nuclear Medicine, Oberdürrbacher Strasse 6, D-97080 Würzburg E-mail: lapa_c@ukw.de phone: +49-931-201-35412 fax: +49-931-201-635000

Received: 2017.04.09; Accepted: 2017.05.08; Published: 2017.07.23

Abstract

^{11}C-methionine (MET) has recently emerged as an accurate marker of tumor burden and disease activity in patients with multiple myeloma (MM). This dual-center study aimed at further corroboration of the superiority of MET as positron emission tomography (PET) tracer for staging and re-staging MM, as compared to ^{18}F-2`-deoxy-2`-fluoro-D-glucose (FDG).

78 patients with a history of solitary plasmacytoma (n=4), smoldering MM (SMM, n=5), and symptomatic MM (n=69) underwent both MET- and FDG-PET/computed tomography (CT) at the University Centers of Würzburg, Germany and Navarra, Spain. Scans were compared on a patient and on a lesion basis. Inter-reader agreement was also evaluated. In 2 patients, tumor biopsies for verification of discordant imaging results were available.

MET-PET detected focal lesions (FL) in 59/78 subjects (75.6%), whereas FDG-PET/CT showed lesions in only 47 patients (60.3%; $p<0.01$), accordingly disease activity would have been missed in 12 patients. Directed biopsies of discordant results confirmed MET-PET/CT results in both cases.

MET depicted more FL in 44 patients (56.4%; $p<0.01$), whereas in two patients (2/78), FDG proved superior. In the remainder (41.0%, 32/78), both tracers yielded comparable results. Inter-reader agreement for MET was higher than for FDG ($\kappa = 0.82$ vs $\kappa = 0.72$).

This study demonstrates higher sensitivity of MET in comparison to standard FDG to detect intra- and extramedullary MM including histologic evidence of FDG-negative, viable disease exclusively detectable by MET-PET/CT. MET holds the potential to replace FDG as functional imaging standard for staging and re-staging of MM.

Key words: PET/CT; ^{11}C-methionine; multiple myeloma; FDG.

Introduction

Multiple myeloma (MM) accounts for approximately 1% of all cancers and around 10% of hematological malignancies [1, 2]. Although MM essentially remains incurable, overall survival has improved significantly over the last decade due to availability of various novel drugs and treatment options. The utility of molecular imaging using positron emission tomography (PET) with the radiolabelled glucose analog [^{18}F]-2`-deoxy-2`-fluoro--D-glucose (FDG) for diagnosis, staging and response

assessment has been demonstrated by several studies [3-7]. Moreover, the new International Myeloma Working Group response criteria include PET-based imaging in the evaluation of minimal residual disease [8]. However, glucose metabolism does not fully reflect the vast heterogeneity of the disease and does not allow for a refined understanding of tumor biology. Furthermore, diffuse bone marrow involvement and a rather low metabolic activity of myeloma can reduce sensitivity of FDG imaging [9]. Due to the rapid uptake and metabolic incorporation of radiolabelled amino acids into newly synthesized immunoglobulins [10], *L*-methyl-[^{11}C]-methionine (MET) has emerged as a promising imaging agent [11]. We previously reported a significantly higher retention of MET in well-characterized myeloma cell lines and patient-derived CD138^{+}-plasma cells and the feasibility of monitoring very early treatment response with MET *in vitro* and *in vivo* [12, 13]. Recently, in initial analyses MET outperformed FDG as a more accurate marker of tumor burden and disease activity [14-16]. This study was aimed to further determine the superiority of MET as PET radiotracer for functional imaging of MM at two different University centers.

Materials and Methods

This prospective study was approved by the local ethics committees of the University of Würzburg (212/13) and the University of Navarra (161/2015). All patients gave written informed consent to FDG- and MET- PET/computed tomography (CT) imaging according to the Declaration of Helsinki. MET was administered under the conditions of the pharmaceutical law (German Medicinal Products Act, AMG §13 2b; RD 1015/2009) according to the German and Spanish law and in accordance with the responsible regulator bodies (Regierung von Oberfranken; AEMPS).

Subjects

78 patients (45 males, 33 females, age 31-82 y, mean 59±10 y, 57 from Würzburg, 21 from Navarra) with a history of solitary plasmacytoma (n=4), smoldering MM (SMM, n=5), and overt MM (n=69) were prospectively enrolled. 17/78 patients were newly diagnosed while the remaining 61 subjects underwent imaging due to suspicion of disease relapse (n=38) or to rule out residual and/or new metabolically active disease (n=23, including plasmacytoma and SMM patients), respectively. At the time of PET/CT scanning, serum free immunoglobulin light chains (FLC; all patients) and the M component were recorded (n=70). Serum chemistry including lactate dehydrogenase (LDH, n=74), albumin (n=75), creatinine (all patients) and β2-microglobulin (β2m, n=68) were also available. Information on degree of bone marrow (BM) infiltration by myeloma cells based on iliac crest biopsy was simultaneously assessed in 54/78 (69.2%) patients. Additionally, interphase molecular cytogenetics based on fluorescence *in situ* hybridization (FISH) was available in 55/78 (70.5%) patients. Presence of del(17p), t(4;14), t(14;16), t(14;20) or chromosome 1 abnormalities were considered as elevated-risk, whereas all other karyotypes were classified as standard risk.

A subgroup of this cohort (32 heavily pre-treated and 11 newly diagnosed patients, all from Würzburg) had previously been published [14].

PET/CT

FDG and MET were synthesized in house with a 16 MeV Cyclotron (Würzburg; GE PETtrace 6; GE Healthcare, Milwaukee, USA) and an 18 MeV Cyclotron (Navarra; Cyclone 18/9, IBA Radiopharma Solutions, Belgium). PET/CT was performed on a PET/CT scanner (Siemens Biograph mCT 64, Siemens, Knoxville, USA, both institutions) within a median interval of 1 day between scans (range, 0-21).

FDG (mean, 303 ± 33 MBq) and MET (mean, 657 ± 147 MBq) were injected intravenously after at least 4h fasting. CT scans were acquired after 60 (FDG) or 20 min. (MET), respectively, using contrast-enhanced (FDG; depending on kidney function; dose modulation with a quality reference of 210 mAs [Würzburg]), non-contrast-enhanced (Care Dose 4D with a quality reference of 120 mAs [Navarra]) or low-dose spiral CT (80 mAs, 120 kV, a 512 × 512 matrix, 5 mm slice thickness, increment of 30 mm/s, rotation time of 0.5 s, and pitch index of 0.8) including the skull to the proximal thighs. Consecutively, PET emission data were acquired in 3D-mode with a 200 × 200 matrix with 2 min (Würzburg) or 3 min (Navarra) emission time per bed position. After decay and scatter correction, PET data were reconstructed iteratively with attenuation correction using a dedicated software (HD. PET, Siemens Esoft, Erlangen, Germany).

Image analysis

Criteria to define lesions as PET-positive by FDG were those previously proposed by Zamagni *et al.* [17], while for MET, positive lesions were visually determined as focally increased tracer retention compared to surrounding normal tissue or contralateral structures as previously described[14]. Presence and number of intra- and extramedullary (EMD) disease as well as location of lesions were recorded. Analysis both on a patient and a lesion basis

was performed.

In order to correlate tracer uptake with BM involvement, the number of intramedullary lesions detected by each tracer was compared to infiltration of malignant myeloma cells, as determined by bone marrow biopsy.

Additionally, to assess the level of inter-reader agreement for presence or absence of disease on a patient basis, the nuclear medicine physicians from each center were blinded for clinical information and read the scans from the other hospital.

PET-directed biopsies and histological assessment

In two patients with discordant results between MET and FDG PET/CT, directed histopathological biopsies were performed in order to evaluate the specificity of the two PET radiolabels.

Statistical analysis

Statistical analyses were performed using PASW Statistics software (version 22.0; SPSS, Inc. Chicago, Illinois, USA). Quantitative values were expressed as mean ± standard deviation or median and range as appropriate. Comparisons of related metric measurements were performed using Wilcoxon-signed rank test. The Chi square- or Fisher exact test was conducted for comparison of frequency data between independent subgroups. For bivariate correlation analyses, Spearman or Pearson correlation coefficients were calculated. Levels of agreement between readers were measured using non-weighted κ statistics. κ values between 0.81 and 1.00 indicate very good agreement, 0.61 and 0.80 indicate good agreement, 0.41 and 0.60 indicate moderate agreement, and 0.21 to 0.4 indicate fair agreement [18]. All statistical tests were performed two-sided and a p-value < 0.05 was considered to indicate statistical significance. No correction for p-values was applied to adjust for multiple tests.

Results

69/78 (88.5%) of the patients investigated presented with symptomatic MM, while the remaining patients suffered from plasmacytoma (n=4, 5.1%) or SMM (n=5, 6.4%). High-risk cytogenetics were present in 25/78 (32.1%) subjects. Information on the degree of iliac BM infiltration with MM plasma cells was available for 54/78 (69.2%) patients and ranged from 0 to 90% (median, 20% plasma cells). Serum FLC ranged from 0.69 to 28.983 mg/l (median, 103.5) and M gradients from 0 to 58.9 g/dl (median, 1.8) Patients´ characteristics are summarized in Table 1 and Supplementary Table 1.

Table 1. Patients´characteristics at the time of PET/CT evaluation

No.	Sex	Age	Myeloma type	Disease duration (months)	M gradient (g/dl)	Involved serum FLC (mg/l)	BM involvement (%)	Previous therapies
Solitary plasmacytoma								
1	f	64	solitary plasmacytoma	PD	0	9.0 (λ)	0	none
2	f	48	solitary plasmacytoma	PD	n/a	4.4	3	none
3	m	31	solitary plasmacytoma	9	0	1.8	0.5	RTx
4	m	32	solitary plasmacytoma	14	n/a	1.7	0,5	CTx
Smoldering Multiple Myeloma (SMM)								
5	m	68	SMM Ig G λ	PD	3.69	8.7 (λ)	n/a	none
6	m	74	SMM Ig G κ	43	21.1	791.5	n/a	none
7	m	44	SMM IgG λ	34	27.44	87.7	n/a	none
8	f	60	SMM Ig G κ	9	8.8	1.2	45	none
9	f	65	SMM Ig G λ	125	1.81	1.7	1	none
Multiple Myeloma (primary diagnosis)								
10	m	76	Ig G κ	PD	3.4	4440 (κ)	40	none
11	f	65	Ig A κ	PD	0	233 (κ)	30	none
12	m	54	Ig A κ	PD	41.3	11.6 (κ)	70	none
13	f	56	Ig A λ	PD	n/a	345 (λ)	25	none
14	m	48	Ig G κ	PD	58.9	48.0 (κ)	n/a	none
15	f	74	Ig G λ	PD	31.9	337 (λ)	n/a	none
16	m	63	LC κ	PD	1.9	14014 (κ)	70	none
17	m	47	LC κ	PD	0	904.9 (κ)	90	none
18	m	62	LC λ	PD	1.8	444.0 (λ)	15	none
19	m	72	Ig G λ	PD	35.4	5297 (λ)	90	none
20	f	62	IgA κ	PD	53.82	33.2	n/a	none
21	m	62	Ig G κ	PD	12.33	259.7	n/a	none
22	f	61	IgG κ	PD	2.47	158	20	none
23	m	37	LC κ	PD	1.9	291	8	none
Multiple Myeloma (re-staging)								
24	f	65	Ig A κ	3	0	498 (κ)	50	CTx
25	m	64	Ig G κ	4	51.1	293 (κ)	40	CTx

26	f	60	Ig G κ	120	16.2	1237 (κ)	n/a	CTx, Auto-Tx
27	m	60	Ig A λ	9	3.5	2525 (λ)	90	CTx, Auto-Tx
28	m	82	Ig A κ	55	n/a	23.0 (κ)	n/a	CTx,
29	m	67	Ig G λ	15	n/a	15.7 (κ)	5	CTx, Auto-Tx
30	m	59	LC κ	7	3.4	n/a	n/a	RTx
31	m	70	Ig G κ	103	23.2	8833 (κ)	n/a	CTx, Auto-Tx
32	f	69	Ig G κ	10	26.4	687 (κ)	n/a	CTx, Auto-Tx
33	f	63	LC κ	32	0	3079 (κ)	n/a	CTx, Auto-Tx
34	f	64	Ig A κ	6	0	27,4 (κ)	0	CTx; Auto-Tx
35	m	56	Ig A κ	32	44.7	0.5 (κ)	50	CTx, Auto-Tx
36	f	62	Ig G κ	11	24.4	254.3 (κ)	15	CTx
37	f	48	Ig A λ	63	6	177.7 (λ)	3	CTx, Auto-Tx
31	m	51	Ig G κ	34	24.6	828.0 (κ)	60	CTx, Auto-Tx
39	m	59	Ig G κ	37	0	5.0 (κ)	0	CTx, Auto-Tx
40	m	59	Ig G κ	4	26.3	551.2 (κ)	40	CTx
41	m	65	Ig G κ	89	10.4	37.8 (κ)	n/a	CTx, Auto-Tx
42	f	65	Ig A κ	12	0	2387 (κ)	90	CTx, Auto-Tx
43	f	39	Ig G λ	58	31.0	97.5 (λ)	n/a	CTx, Auto-Tx
44	f	68	Ig G λ	31	29.8	1673 (λ)	35	CTx, Auto-Tx
45	m	73	Ig G κ	72	4.7	25100 (κ)	70	CTx, Auto-Tx
46	m	62	Ig G κ	199	13.0	14015 (κ)	20	CTx, Auto-Tx
47	m	62	LC λ	47	0	240.8 (λ)	5	CTx, Auto-Tx
48	f	53	LC κ	122	0	99.0 (κ)	15	CTx, Auto-Tx
49	m	63	LC λ	6	0	12.4 (λ)	0	CTx
50	f	63	Ig G κ	22	47.5	1907 (κ)	30	CTx, Auto-Tx
51	m	63	Ig G κ	86	4.1	535.0 (κ)	n/a	CTx, Auto-Tx
52	m	60	LC λ	22	0	124.2 (λ)	20	CTx, Auto-Tx
53	f	63	LC λ	23	0	1876 (λ)	10	CTx, Auto-Tx
54	f	49	Ig A λ	72	0	30.8 (λ)	0	CTx, Auto-Tx
55	f	40	LC κ	39	0	50.0 (κ)	n/a	CTx, Auto-Tx
56	f	46	Ig G λ	34	5.4	107.9 (λ)	n/a	CTx, Auto-Tx
57	m	64	Ig G λ	64	0	1114 (λ)	0	CTx, Auto-Tx
58	m	48	Ig G λ	10	0	16.1 (λ)	0	CTx
59	m	62	Ig G κ	109	16.06	70.9	n/a	CTx
60	m	74	Ig A λ	83	0.88	28983 (λ)	50	CTx, Auto-Tx
61	m	61	LC κ	23	0	2947	60	CTx
62	f	62	Ig G κ	39	1.65	955	10	CTx, Auto-Tx
63	f	66	LC λ	10	0	11.5 (λ)	n/a	CTx, Auto-Tx
64	m	41	asecretory	19	0	n/a	n/a	CTx, Auto-Tx
65	f	57	LC κ	64	1.77	5,1	60	CTx, Auto-Tx
66	m	62	Ig G κ	122	0	1.3	0,5	CTx, Auto-Tx
67	f	61	Ig G κ	124	1.7	12.3	27	CTx, Auto-Tx
68	m	44	Ig G κ	3	0.9	0.7	4	CTx
69	f	65	LC λ	29	1.5	2.8	6	CTx, Auto-Tx
70	m	63	Ig G κ	44	1.8	137	20	CTx, Auto-Tx
71	m	73	Ig G κ	106	0.71	24.9	40	CTx
72	f	65	LC κ	47	0.18	87.4	19	CTx, Auto-Tx
73	m	46	Ig G κ	6	0	0.4	5	CTx, Auto-Tx
74	f	68	Ig G κ	46	0.25	3.5	n/a	CTx, Auto-Tx
75	m	51	Ig G κ	24	0.41	7.2	n/a	CTx
76	m	50	Ig G κ	32	n/a	28.6	4	CTx, RTx
77	m	56	Ig D λ	40	n/a	123	n/a	CTx, Auto-Tx
78	f	48	Ig G κ	57	n/a	1	3	CTx, Auto-Tx

m = male. f = female. Disease duration is given in months. PD = primary diagnosis. CTx = chemotherapy including novel agents. LC = light chain. RTx = radiotherapy. SMM = smoldering multiple myeloma. Auto-Tx = autologous stem cell transplantation. n/a = information not available.

Patient-based analysis

In PET/CT examinations with MET, MM lesions were detected in 59/78 patients (75.6%). In contrast, FDG did not identify any focal lesion in 31 patients (FDG-positive lesions in 47/78 patients, 60.3%; $p<0.01$). The 19 MET-negative patients corresponded to either cases in complete response (CR; n=13) or very good partial response (VGPR; n= 2) or cases with SMM (n=4). Of note, the remaining patient with SMM (patient #60) revealed increased MET uptake throughout the skeleton, whereas FDG-PET showed negative results (Figure 1).

Additionally, MET identified extramedullary lesions in 15/78 patients (19.2%), whereas FDG identified 13/78 patients (p=n.s.) with EMD (16.7%). These extramedullary lesions corresponded to: soft tissue (9/78 [MET] vs. 7/78 [FDG]); lymph nodes (8/78 [MET] vs 7/78 [FDG]), lung (2/78 [MET] vs. 2/78 [FDG] and liver (0/78 [MET] vs. 1/78 [FDG]). Regarding intramedullary MM, MET revealed involvement of the appendicular skeleton in 52/78

patients (66.7%), whereas 14 cases were missed with FDG (FDG-positive lesions in 38/78 patients, 48.7%) (Supplementary Table 2).

Inter-reader agreement

Only one patient was not available for the inter-reader agreement evaluation due to technical reasons. Reproducibility of overall scan results was very good for MET scans with an agreement between readers in 72 of 77 scans. (κ = 0.82, 95% confidence interval [CI] 0.66-0.97). For FDG inter-reader agreement was good with consensus reached in 67 of 77 examinations (κ = 0.72, 95% CI 0.56-0.88).

Lesion-based analysis

Imaging with MET identified more focal lesions than FDG in 44 patients (44/78, 56.4%, p<0.01), whereas FDG proved superior in only 2/78 (2.6%) cases (Figure 2). In the remaining 32/78 (41.0%) patients, an equal number of MM manifestations (identical lesions) was detected with both tracers.

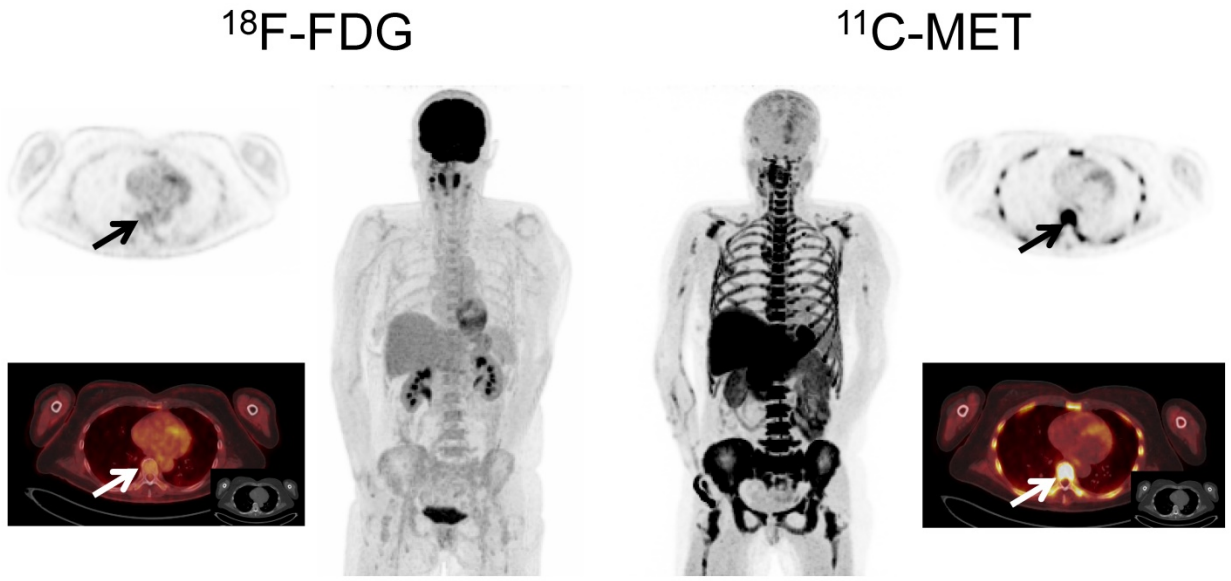

Figure 1. Display of a patient (patient #8) with Ig G κ SMM. Imaging with both tracers was performed on the same day. Whereas PET/CT with FDG did not depict hypermetabolic foci suspicious for active MM, MET demonstrated increased tracer uptake throughout the skeleton. Bone marrow biopsy revealed 45% clonal plasma cells. Blood tests showed an IgG κ M-spike of 8.6 g/dl, free light chain (FLC) κ levels of 1.22 mg/dl, and FLC λ levels of 0.13 mg/dl (ratio κ/λ= 9.38). Bence-Jones proteinuria was 191 mg/24 h-collected urine. The patient was diagnosed of high-risk smoldering MM and started treatment in a Spanish myeloma group clinical trial. After induction and consolidation treatment, she is in stringent complete response with MRD negativity as assessed by flow cytometry.

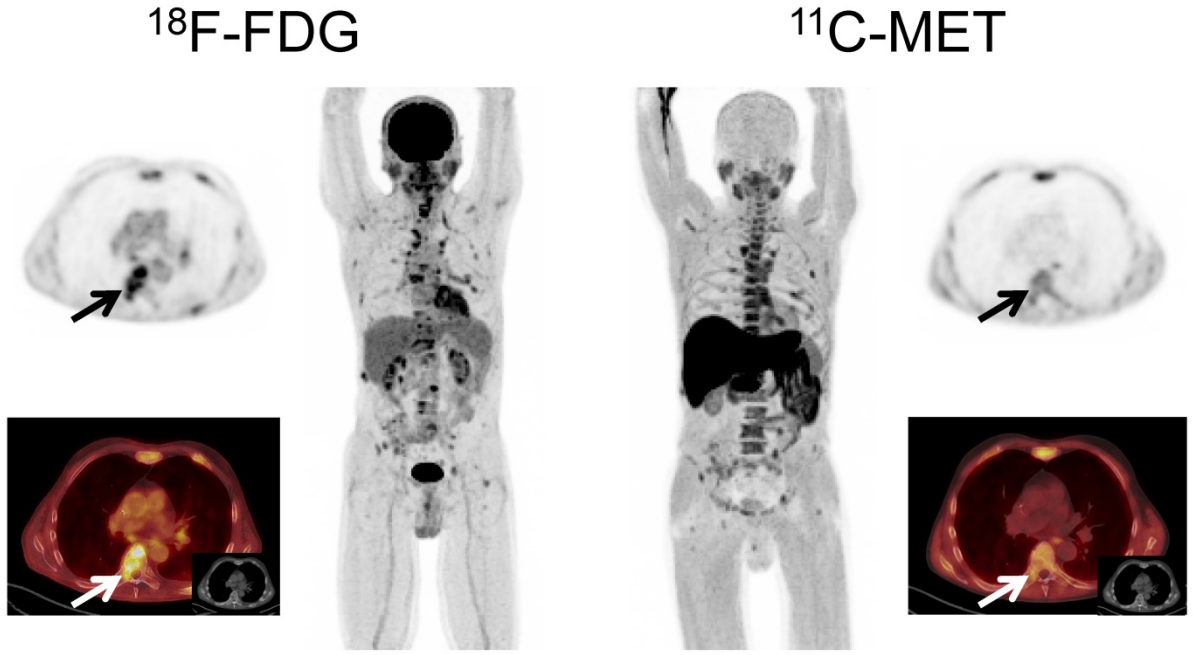

Figure 2. Display of a patient (patient #57) with a history of Ig G λ MM. Imaging with both tracers was performed within 6 days. PET/CT with FDG depicted multiple hypermetabolic foci consistent with active MM which were partly missed by MET (transaxial slice of thoracic vertebra Th 7, arrows).

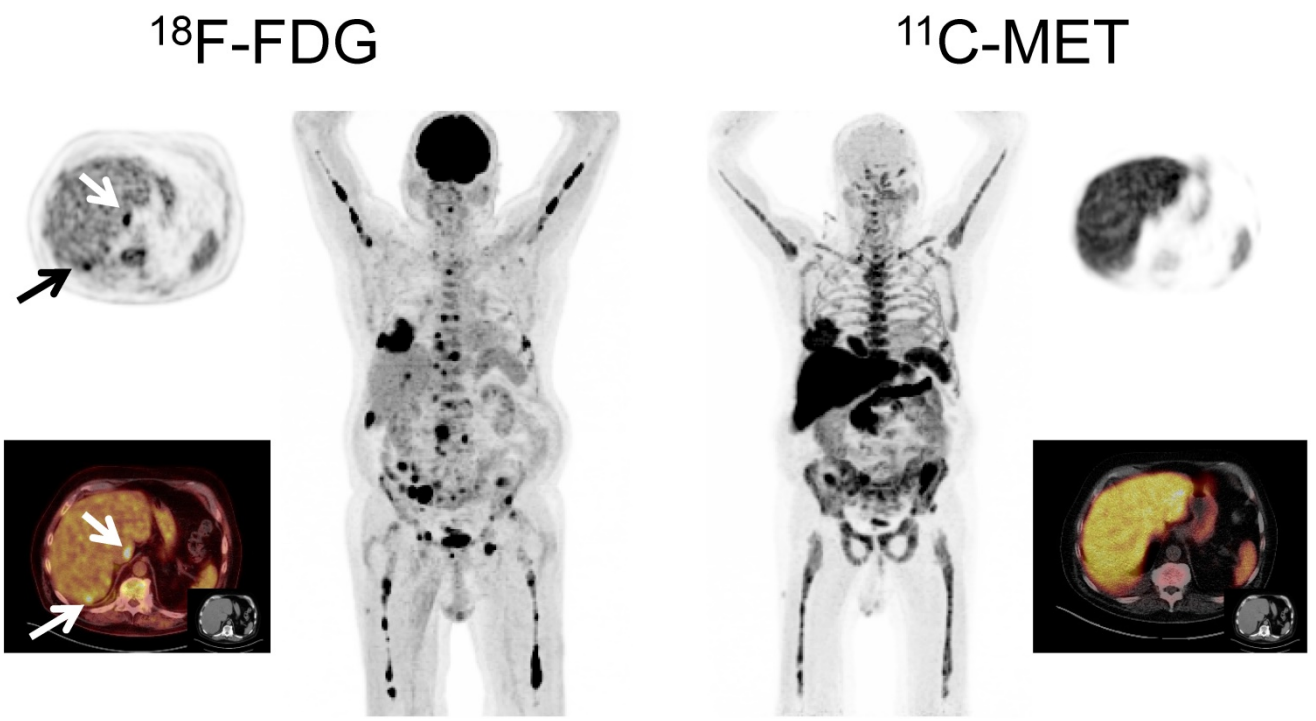

Figure 3. Display of a patient (patient #60) with a history of Ig A λ MM. Imaging with both tracers depicted multiple hypermetabolic foci consistent with active MM. However, due to high physiologic uptake, extramedullary liver lesions were missed by MET-PET (arrows).

MET-PET/CT detected ≥ 20 FL in 52 out of the 59 positive patients (88.1%): 11/59 (18.6%) had ≥ 20 focal lesions detected, 8/59 patients (13.6%) ≥50 and 33/59 patients (55.9%) ≥100 FL. The remaining 7/59 (11.9%) patients had less than 20 FL. With FDG, 21/47 (44.7%) subjects had <20 FL, 11/47 (23.4%) ≥20, 4/47 (8.5%) ≥50 and 11/47 (23.4%) ≥100 FL.

Interestingly, in 7/15 patients (46.7%) with EMD, MET detected lesions which were missed by FDG, whereas FDG outperformed MET in a single patient with hepatic EMD (Figure 3). In numbers, FDG detected a total of 44 EMD foci (soft tissue, n=20; lymph nodes, n=18; liver, n=4; lung, n=2), whereas MET depicted 72 lesions ($p<0.01$) in soft tissue (n=43), lymph nodes (n=24), and lungs (n=5). The lesions exclusively visualized by MET were found in soft tissue (n=23), lymph nodes (n=6), and lungs (n=3) (supplementary table 2).

Correlation of tracer uptake with bone marrow involvement

In the 54/78 (69.2%) patients in whom BM infiltration was histologically assessed by iliac crest biopsies or aspirates, the number of intramedullary lesions detected by PET imaging with either tracer correlated well with histologic plasma cell infiltration. Correlation with the histological findings was stronger for MET-PET (Spearman´s r=0.832) than for FDG-PET (Spearman´s r=0.635).

PET-directed biopsies and histopathological assessment

In order to confirm the specificity of MET-PET, directed histopathological biopsies were performed in two patients with discordant results between FDG-PET and MET-PET. In one case with FDG^+ and MET^- imaging (patient # 67, Figure 4), the guided biopsy did not show plasma cell infiltration whereas in the second case (MET^+/FDG^-, patient # 62, Figure 5), infiltration of clonal plasma cells was confirmed. Accordingly, in both cases the biopsy results were concordant with the MET-PET findings.

Discussion

This study aimed at further validation of the radiolabelled amino acid MET for functional imaging of multiple myeloma. The superiority of MET over FDG was confirmed with concordant results in both University centers. Most interestingly, in two cases in which PET-guided biopsies were performed to clarify discordant PET imaging results the histopathological examination confirmed the MET based findings, with clonal plasma cells being present in the MET^+/FDG^- but being absent in the MET^-/FDG^+ lesion. This adds evidence that this radiolabel has higher sensitivity and specificity for myeloma lesions than FDG.

In parallel with previously published data demonstrating higher sensitivity [14-16], MET provided more accurate information on the disease

burden in the majority of patients and demonstrated higher inter-reader agreement. Based on PET-derived SUV, it also demonstrated a better correlation with histologic plasma cell infiltration as derived from iliac crest biopsy samples in comparison to FDG.

Of note, MET demonstrated more myeloma lesions not only in intramedullary, but also in extramedullary disease. In almost half of the patients with EMD, exclusively MET^+ lesions could be depicted. The biologically underlying implications are not yet fully understood. Further studies investigating samples from targeted biopsies (MET^+/FDG^+; MET^-/FDG^+; MET^+/FDG^-) are needed to derive a better estimate of the prognosis and refractoriness to treatment by the type of lesions displaying divergent MET and FDG uptake.

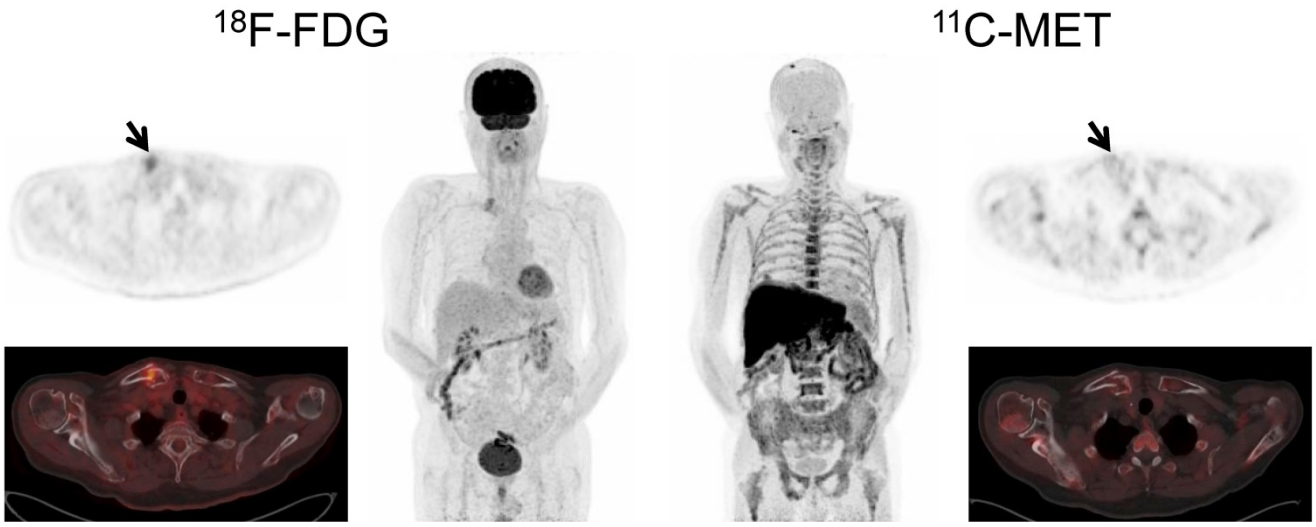

Figure 4. Display of a patient (patient #71) with a history of Ig G κ MM after treatment initiation with lenalidomide and dexamethasone. The patient was referred for further evaluation of a painful, growing lesion in the proximal third of the right clavicle. The lesion demonstrated focal FDG uptake. In contrast, MET-PET was negative (arrows). Biopsy was performed and no tumor infiltration was demonstrated, consistent with a benign fracture. MET-PET additionally revealed partial response with inhomogeneous, focally increased tracer uptake of the axial as well as appendicular skeleton, whereas FDG-PET did not depict hypermetabolic foci suspicious for active MM in these locations.

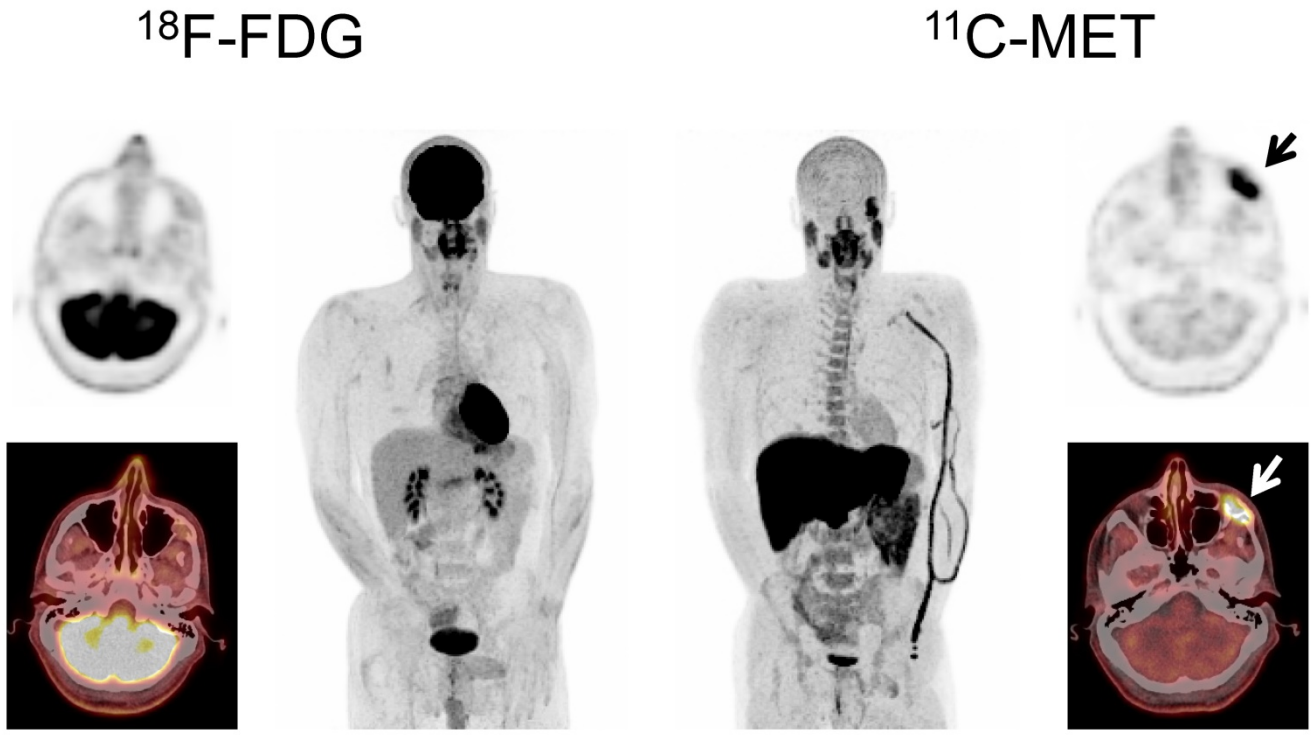

Figure 5. Display of a patient (patient #3) with a history of solitary plasmacytoma treated with radiotherapy. Imaging with both tracers was performed on the same day. Whereas PET/CT with FDG did not depict hypermetabolic foci suspicious for active MM, MET demonstrated focally increased tracer uptake in the left zygomatic bone (arrows). Biopsy confirmed monoclonal plasma cell infiltration.

MET-PET was negative in most patients with MM in CR/VGPR and smoldering myeloma. Interestingly, a single patient with SMM presented with MET^+/FDG^- disease (Figure 2). Whereas it is too early to comment on the suitability of MET-PET for the identification of high-risk SMM patients, tracer uptake might reflect true active myeloma [19] and might be potentially of use to identify patients in conversion from asymptomatic disease stages to early, treatment demanding MM. While the value of blood markers and magnetic resonance imaging (MRI) for the identification of high-risk SMM were recently established and incorporated in the MM diagnostic criteria of the International Myeloma Working Group [20, 21], the role of PET/CT in SMM -despite first reports on the general suitability of FDG [22-24]- has not yet been comprehensively elucidated. A study on the diagnostic and prognostic value of FDG-, MET- and C-X-C motif chemokine receptor 4- (CXCR4-) directed PET [25-27] to determine the role of PET imaging in MM is currently ongoing in Würzburg.

Additionally, another potential application of MET-PET might be considered in patients with (assumed) solitary plasmacytoma. Given the fact that a substantial proportion of patients develop MM within 2 years after radiotherapy of the solitary lesion [28], MET-PET performed at the initial presentation could contribute to detection of additional viable myeloma lesions and therefore, identify a patient subgroup benefitting from systemic therapy. Future research will clarify the role of MET-PET in this setting.

As a potential drawback of the amino acid tracer, reduced sensitivity within the liver has been considered [29]. Indeed, in a single patient with hepatic MM involvement, MET did not detect the lesions due to the high physiologic uptake. However, given the broad availability of combined PET/CT imaging, this drawback should be overcome by the simultaneously acquired anatomic information. Future studies should address the prognostic value of MET in comparison to FDG and the performance of the tracer in early response assessment. A shortcoming of the present study is the limited number of patients with biopsy for verification of discordant FDG and MET imaging results. Although tumor biopsies from sites with discordant biologic behaviour (MET^+/FDG^-) have been carried out for the first time in this study, the underlying biological implications of these discrepant cases remain to be elucidated. Furthermore, another distinct pattern of myeloma lesions has been shown by receptor-directed PET targeting CXCR4 [26, 30, 31]. A current PET-guided biopsy project at our centers aims at a more elaborated analysis of biologically different myeloma lesions in order to gain further insight into MM heterogeneity. Additionally, a comparison of MET with other metabolic tracers like ^{11}C-choline or ^{11}C-acetate is currently ongoing.

Of note, the phenomenon of about 10% of FDG-PET "false-negative" patients due to low expression of hexokine-2 has been recently reported and might at least mechanistically explain the differences observed between the two PET tracers [32]. Since these patients cannot be monitored by FDG-PET, MET might overcome this limitation and aid in therapy monitoring in this relevant sub-group of patients.

Overall, this study adds sustained evidence on the suitability of MET-PET for assessment of myeloma tumor burden. It indicates superiority over standard FDG-based imaging. Importantly we report the first evidence of histologically proven FDG-negative MM detectable by MET. Taken together, it can be hypothesized that MET-PET adds significant benefit to our diagnostic armamentarium in MM. Further clinical trials including a comprehensive evaluation of the prognostic and predictive value of this technology are clearly needed.

Conclusion

In conclusion, this study presents –for the first time- histologic proof of FDG-negative, viable MM detectable by MET-PET/CT. MET holds the potential to replace FDG as functional imaging standard for MM.

Acknowledgements

We thank Dirk O. Mügge for his kind assistance in data analysis. This work was supported by the Wilhelm-Sander-Stiftung (grant no. 2013.906.1), the Ministry of Economy and Competitiveness (PI 16/00225), and the Ministry of Science and Innovation, Government of Spain (grant no. ADE 10/00028).

Authorship contributions

Initials: Constantin Lapa (CL), Maria J. Garcia-Velloso (MGV), Katharina Lückerath (KL), Samuel Samnick (SSa), Martin Schreder (MS), Paula Rodriguez Otero (PRO), Jan-Stefan Schmid (JSS), Stefan Knop (SK), Ken Herrmann (KH), Andreas K. Buck (AKB), Hermann Einsele (HE), Jesus San-Miguel (JSM), Klaus Martin Kortüm (KMK)

Conception and design: CL, MGV, KL, JSM, HE, KMK

Development of methodology: CL, KL, SSa, MS, PRO, JSS

Acquisition of data: CL, MGV, MS, JSS, SK, KH, KMK

Analysis and interpretation of data: CL, MGV, KL,

SSa, JSS, KH, AKB
Writing, review and/or revision of the manuscript: all authors
Administrative, technical, or material support: SSa, AKB, JSM
Supervision: AKB, JSM, HE, KH

Supplementary Material

Supplementary tables.
http://www.thno.org/v07p2956s1.pdf

Competing Interests

The authors have declared that no competing interest exists.

References

1. Phekoo KJ, Schey SA, Richards MA, Bevan DH, Bell S, Gillett D, et al. A population study to define the incidence and survival of multiple myeloma in a National Health Service Region in UK. Br J Haematol. 2004; 127: 299-304.
2. Siegel R, Naishadham D, Jemal A. Cancer statistics, 2013. CA: a cancer journal for clinicians. 2013; 63: 11-30.
3. Durie BG. The role of anatomic and functional staging in myeloma: description of Durie/Salmon plus staging system. Eur J Cancer. 2006; 42: 1539-43.
4. Durie BG, Waxman AD, D'Agnolo A, Williams CM. Whole-body (18)F-FDG PET identifies high-risk myeloma. J Nucl Med. 2002; 43: 1457-63.
5. Bartel TB, Haessler J, Brown TL, Shaughnessy JD, Jr., van Rhee F, Anaissie E, et al. F18-fluorodeoxyglucose positron emission tomography in the context of other imaging techniques and prognostic factors in multiple myeloma. Blood. 2009; 114: 2068-76.
6. Hillner BE, Siegel BA, Shields AF, Liu D, Gareen IF, Hunt E, et al. Relationship between cancer type and impact of PET and PET/CT on intended management: findings of the national oncologic PET registry. J Nucl Med. 2008; 49: 1928-35.
7. Lapa C, Luckerath K, Malzahn U, Samnick S, Einsele H, Buck AK, et al. 18 FDG-PET/CT for prognostic stratification of patients with multiple myeloma relapse after stem cell transplantation. Oncotarget. 2014; 5: 7381-91.
8. Kumar S, Paiva B, Anderson KC, Durie B, Landgren O, Moreau P, et al. International Myeloma Working Group consensus criteria for response and minimal residual disease assessment in multiple myeloma. Lancet Oncol. 2016; 17: e328-46.
9. Terpos E, Moulopoulos LA, Dimopoulos MA. Advances in imaging and the management of myeloma bone disease. J Clin Oncol. 2011; 29: 1907-15.
10. Hammerton K, Cooper DA, Duckett M, Penny R. Biosynthesis of immunoglobulin in human immunoproliferative diseases. I. Kinetics of synthesis and secretion of immunoglobulin and protein by bone marrow cells in myeloma. J Immunol. 1978; 121: 409-17.
11. Dankerl A, Liebisch P, Glatting G, Friesen C, Blumstein NM, Kocot D, et al. Multiple Myeloma: Molecular Imaging with 11C-Methionine PET/CT--Initial Experience. Radiology. 2007; 242: 498-508.
12. Luckerath K, Lapa C, Spahmann A, Jorg G, Samnick S, Rosenwald A, et al. Targeting paraprotein biosynthesis for non-invasive characterization of myeloma biology. PloS one. 2013; 8: e84840.
13. Luckerath K, Lapa C, Albert C, Herrmann K, Jorg G, Samnick S, et al. 11C-Methionine-PET: a novel and sensitive tool for monitoring of early response to treatment in multiple myeloma. Oncotarget. 2015; 6: 8418-29.
14. Lapa C, Knop S, Schreder M, Rudelius M, Knott M, Jorg G, et al. 11C-Methionine-PET in Multiple Myeloma: Correlation with Clinical Parameters and Bone Marrow Involvement. Theranostics. 2016; 6: 254-61.
15. Nakamoto Y, Kurihara K, Nishizawa M, Yamashita K, Nakatani K, Kondo T, et al. Clinical value of (1)(1)C-methionine PET/CT in patients with plasma cell malignancy: comparison with (1)(8)F-FDG PET/CT. Eur J Nucl Med Mol Imaging. 2013; 40: 708-15.
16. Okasaki M, Kubota K, Minamimoto R, Miyata Y, Morooka M, Ito K, et al. Comparison of (11)C-4'-thiothymidine, (11)C-methionine, and (18)F-FDG PET/CT for the detection of active lesions of multiple myeloma. Ann Nucl Med. 2015; 29: 224-32.
17. Zamagni E, Patriarca F, Nanni C, Zannetti B, Englaro E, Pezzi A, et al. Prognostic relevance of 18-F FDG PET/CT in newly diagnosed multiple myeloma patients treated with up-front autologous transplantation. Blood. 2011; 118: 5989-95.
18. Altman DG. Practical statistics for medical research. Boca Raton, Fla.: Chapman & Hall/CRC; 1999.
19. Okubo S, Zhen HN, Kawai N, Nishiyama Y, Haba R, Tamiya T. Correlation of L-methyl-11C-methionine (MET) uptake with L-type amino acid transporter 1 in human gliomas. J Neurooncol. 2010; 99: 217-25.
20. Rajkumar SV, Dimopoulos MA, Palumbo A, Blade J, Merlini G, Mateos MV, et al. International Myeloma Working Group updated criteria for the diagnosis of multiple myeloma. Lancet Oncol. 2014; 15: e538-48.
21. Rajkumar SV, Landgren O, Mateos MV. Smoldering multiple myeloma. Blood. 2015; 125: 3069-75.
22. Zamagni E, Nanni C, Gay F, Pezzi A, Patriarca F, Bello M, et al. 18F-FDG PET/CT focal, but not osteolytic, lesions predict the progression of smoldering myeloma to active disease. Leukemia. 2016; 30: 417-22.
23. Siontis B, Kumar S, Dispenzieri A, Drake MT, Lacy MQ, Buadi F, et al. Positron emission tomography-computed tomography in the diagnostic evaluation of smoldering multiple myeloma: identification of patients needing therapy. Blood Cancer J. 2015; 5: e364.
24. Bhutani M, Turkbey B, Tan E, Korde N, Kwok M, Manasanch EE, et al. Bone marrow abnormalities and early bone lesions in multiple myeloma and its precursor disease: a prospective study using functional and morphologic imaging. Leuk Lymphoma. 2016; 57: 1114-21.
25. Herrmann K, Lapa C, Wester HJ, Schottelius M, Schiepers C, Eberlein U, et al. Biodistribution and radiation dosimetry for the chemokine receptor CXCR4-targeting probe 68Ga-pentixafor. J Nucl Med. 2015; 56: 410-6.
26. Philipp-Abbrederis K, Herrmann K, Knop S, Schottelius M, Eiber M, Luckerath K, et al. In vivo molecular imaging of chemokine receptor CXCR4 expression in patients with advanced multiple myeloma. EMBO Mol Med. 2015; 7: 477-87.
27. Demmer O, Gourni E, Schumacher U, Kessler H, Wester HJ. PET imaging of CXCR4 receptors in cancer by a new optimized ligand. ChemMedChem. 2011; 6: 1789-91.
28. de Waal EG, Leene M, Veeger N, Vos HJ, Ong F, Smit WG, et al. Progression of a solitary plasmacytoma to multiple myeloma. A population-based registry of the northern Netherlands. Br J Haematol. 2016; 175: 661-667.
29. Mesguich C, Zanotti-Fregonara P, Hindie E. New Perspectives Offered by Nuclear Medicine for the Imaging and Therapy of Multiple Myeloma. Theranostics. 2016; 6: 287-90.
30. Lapa C, Schreder M, Schirbel A, Samnick S, Kortum KM, Herrmann K, et al. [68Ga]Pentixafor-PET/CT for imaging of chemokine receptor CXCR4 expression in multiple myeloma - Comparison to [18F]FDG and laboratory values. Theranostics. 2017; 7: 205-12.
31. Lapa C, Schirbel A, Samnick S, Luckerath K, Kortum KM, Knop S, et al. The gross picture: intraindividual tumour heterogeneity in a patient with nonsecretory multiple myeloma. Eur J Nucl Med Mol Imaging. 2017; 44: 1097-8.
32. Rasche L, Angtuaco E, McDonald JE, Buros A, Stein C, Pawlyn C, et al. Low expression of hexokinase-2 is associated with false-negative FDG-positron emission tomography in multiple myeloma. Blood. 2017; [Epub ahead of print].